PRECLINICAL AND CLINICAL SPECTROSCOPY – Note

Magnetic Resonance in Medicine 77:520–528 (2017)

Transverse Relaxation of Selectively Excited Metabolites in Stroke at 21.1 T

Jens T. Rosenberg,[1]* Noam Shemesh,[2] Jose A. Muniz,[1,3] Jean-Nicolas Dumez,[4] Lucio Frydman,[1,5] and Samuel C. Grant[1,3]

Purpose: This study seeks to evaluate in vivo T_2 relaxation times of selectively excited stroke-relevant metabolites via ^{1}H relaxation-enhanced magnetic resonance spectroscopy (RE-MRS) at 21.1 T (900 MHz).

Methods: A quadrature surface coil was designed and optimized for investigations of rodents at 21.1 T. With voxel localization, a RE-MRS pulse sequence incorporating the excitation of selected metabolites was modified to include a variable echo delay for T_2 measurements. A middle cerebral artery occlusion (MCAO) animal model for stroke was examined with spectra taken 24 h post occlusion. Fourteen echo times were acquired, with each measurement completed in less than 2 min.

Results: The RE-MRS approach produced high-quality spectra of the selectively excited metabolites in the stroked and contralateral regions. T_2 measurements reveal differential results between these regions, with significance achieved for lactic acid.

Conclusion: Using the RE-MRS technique at ultra-high magnetic field and an optimized quadrature surface coil design, full metabolic T_2 quantifications in a localized voxel is now possible in less than 27 min. **Magn Reson Med 77:520–528, 2017. © 2016 International Society for Magnetic Resonance in Medicine**

Key words: ultrahigh field MRI; 21.1 T MRS; metabolites; stroke; T_2; relaxation

INTRODUCTION

The results of a cerebral ischemia and subsequent metabolic, cellular, and system dysfunctions can result in severe neurological deficits (1). To identify treatment options and predict outcomes, it is crucial to develop methods that can track stroke and its evolution regionally within a lesion. Complementing the spatial information resolved by MRI, which is the modality of choice in stroke research (2–4), magnetic resonance spectroscopy (MRS) is capable of providing highly informative, quantifiable biochemical information on localized cerebral metabolites. In stroke, creatine (Cre) and lactic acid (Lac) are of particular interest for their involvement in bioenergetics, choline (Cho) for its participation in membrane synthesis, and N-acetylaspartate (NAA) for its role in osmotic regulation of neurons (5). Probing these metabolites can convey information about the underlying events in afflicted tissue. For example, reductions in NAA levels are associated with neuronal viability, whereas Lac elevation results from underlying anaerobic glycolysis (6,7). Indeed, noninvasive MRS studies revealed changes in concentration of up to 17 metabolites after ischemic stroke (6,8,9).

Aside from the altered metabolic concentrations associated with stroke, longitudinal (T_1) and transverse (T_2) relaxation times also have been identified as interesting targets that may be able to reflect the complex cascade of events and tissue compartment changes following the disruption of cerebral blood flow (10–13). Transverse relaxation times T_2 and T_2^* (14–16) are particularly interesting features as they reflect contributions from different events. Apparent T_2 and T_2^* relaxation can be compartment and field-dependent, partly because of susceptibility-induced gradients (17) that increase with magnetic field strengths (18). Whereas water is present in nearly every compartment of the targeted tissue and its apparent transverse relaxation may be affected by a multitude of factors, metabolites may be compartmentalized differently and more selectively. Thus, metabolic transverse relaxation rates for ischemic conditions might be affected to different extents than that of water.

^{1}H MRS is usually collected by a broadband excitation that follows water suppression. Recently, a different approach for generating MR spectra has been reported (19), making use of highly spectrally selective excitations that target only specific resonances of interest. The spectral selectivity of the pulses is used to excite, for example, Lac, total Cre (tCre), total Cho (tCho) and NAA, while avoiding water perturbations and minimizing the effects on apparent metabolic T_1 through bulk water exchange. The potential built-in refocusing of scalar (J) couplings (eg, Lac in this study) together with intrinsically shorter apparent metabolic T_1s bestows

[1]The National High Magnetic Field Laboratory, Florida State University, Tallahassee, Florida, USA.

[2]Champalimaud Neuroscience Programme, Champalimaud Centre for the Unknown, Lisbon, Portugal.

[3]Department of Chemical & Biomedical Engineering, FAMU-FSU College of Engineering, Florida State University, Tallahassee, Florida, USA.

[4]French National Centre for Scientific Research, Institute de Chime des Substances Naturelles, Gif-sur-Yvette, France.

[5]Department of Chemical Physics, Weizmann Institute of Science, Rehovot, Israel.

*Correspondence to: Jens T. Rosenberg, The National High Magnetic Field Laboratory, CIMAR, 1800 E. Paul Driac Dr., Tallahassee, FL 32310; Email: rosenberg@magnet.fsu.edu

Correction added after online publication 12 February 2016. The author corrected the locations for affiliations 1 and 3. The caption to figure 4 was corrected to clarify images c and d. Other minor typographical and grammatical corrections were made throughout the text.

Received 8 July 2015; revised 11 December 2015; accepted 27 December 2015

DOI 10.1002/mrm.26132

Published online 1 February 2016 in Wiley Online Library (wileyonlinelibrary.com).

© 2016 International Society for Magnetic Resonance in Medicine

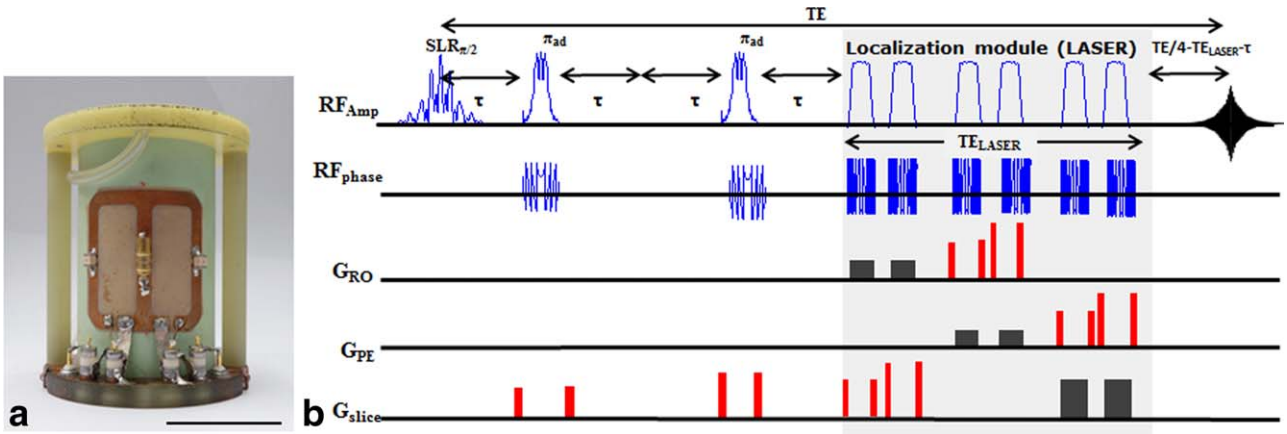

FIG. 1. Coil (a) and pulse sequence (b) employed in this study for T_2 measurements at 21.1 T. (a) Photograph of the coil mounted to a cylindrical former, with the tuning and matching capacitors on the bottom and a variable capacitor placed at the center of the common conductor. The two fixed chip capacitors on each side are 0.9 pF. Scale bar is 3 cm. (b) RE-MRS sequence incorporating a T_2-encoding variable delay τ, $\pi/2$ SLR excitation, and limited-bandwidth adiabatic π refocusing pulses followed by a 3D LASER localization module incorporating crusher gradients (shown in red).

these relaxation-enhanced (RE) MRS data with high fidelity (19). This spectral selectivity can be endowed with spatial selectivity so that voxel-selective RE-MRS studies can be performed in vivo (13,20). At ultra-high fields, these sequences benefit from remarkable signal-to-noise ratio (SNR) per unit time and undistorted baselines, which in turn facilitate the measurement of potential novel biomarkers, such as those reporting a stroke outcome and severity (13,20).

This study describes and characterizes in detail a previously reported T_2-weighted RE-MRS sequence (20), working with an optimized quadrature surface coil designed for 21.1 T (900 MHz), which enable the rapid measurements of metabolic transverse relaxation at this field. Using a significant animal cohort ($n=8$) and building upon preliminary RE-MRS evidence at high field displayed in previous work (13,20), the present study provides a detailed investigation of transverse relaxation at 21.1 T for tCre, tCho, Lac, and NAA following ischemic stroke. These metabolic T_2 values are compared with water T_2 measurements at 21.1 T and to metabolic T_2 measurements performed at lower fields. Additionally, a detailed evaluation of the optimized quadrature coil design is provided to demonstrate the required B_1 coverage and coil efficiency necessary to execute the multiband radiofrequency (RF) pulses required for the RE-MRS sequence. The results demonstrate undistorted, high-sensitivity spectra generated over short-signal averaging times, even when echo times (TE) exceeded 250 ms. Using this technique, relatively long apparent T_2 values were measured at 21.1 T for the in vivo metabolites. These transverse decay times are pooled with results that in normal and stroked animals have been measured at other field strengths (10,11,14,21–25), and show an overall decrease in T_2 relaxation times with increasing field strength.

METHODS

All data were acquired using the ultra-wide bore 21.1T, 900-MHz vertical magnet built at the National High Magnetic Field Laboratory (26). The magnet is equipped with a Bruker Avance III console (Bruker-Biospin, Billerica, Massachusetts) and imaging gradients (Resonance Research, Billerca, Massachusetts) with a peak gradient strength of 600 mT/m. All animal use and surgical procedures were approved by the Florida State University (FSU) Animal Care and Use Committee (ACUC).

RF Coil Design and Implementation

The RF coil design consisted of a homebuilt double-saddle quadrature surface coil resonant at 900 MHz. The coil was built to accommodate the head of large in vivo rodents (up to 350 g). As shown in Figure 1a, this coil consists of two copper loops with a common center conductor and adhered to a 36-mm-diameter fiberglass epoxy former, resulting in an overall azimuthal coverage of approximately 100° from a 30×32 mm surface. The two saddle-shaped RF channels (Fig. 1a) were decoupled electrically by a single variable capacitor placed at the center of the common conductor. A shared capacitance (0.9-pF chip capacitors) was evenly distributed along with variable tuning and matching capacitors (0.8–8.0 pF range). To achieve a transceiver quadrature design, an external 90° hybrid coupler (R&D Microwaves, Boonton, New Jersey) was used to split/combine the RF channels. The probe also was designed to provide continuous anesthesia together with oxygen through a bite bar from which the animal was suspended. The performance of the quadrature coil was evaluated in terms of Q values with a physiologically relevant sample and a rat of representative weight. B_1 flip maps were acquired on a polyethylene glycol phantom and in vivo on rodents, following double-angle methods from Cunningham et al (27).

In Vivo Stroke Model

Eight juvenile male Sprague-Dawley rats weighing between 230–300 g were used in this study. After anesthetizing with isoflurane (Baxter, Deerfield, Illinois) in 100% oxygen, an ischemic stroke was introduced by a transient middle cerebral artery occlusion (MCAO) as described previously (28–30). Briefly, the internal carotid artery and external carotid artery were exposed, and a rubber-coated filament (Doccol, Sharon, Massachusetts) was placed into the

external carotid artery and guided 1.9 cm into the ICA until the middle cerebral artery was blocked. Occlusion was sustained for 1.5 h, followed by re-anesthetization and removal of the filament. The animals were imaged 24 h following the occlusion with no mortalities documented during the course of the experiments.

MRI Sequence

A localized RE-MRS sequence (Fig. 1b) was used (20), accommodating T_2 relaxation measurements for four target metabolites: Lac, NAA, tCre, and tCho. These metabolites were excited by spectrally selective excitation and refocusing pulses targeted to their respective methyl resonances. These polychromatic 8-ms-long band-selective and phase-modulated pulses were designed based on the Shinnar-LeRoux (SLR) algorithm (19,31), creating short bandwidths. Passbands were 72 Hz for Lac and NAA, and 252 Hz for tCre/tCho with stopbands of 180 Hz between Lac-NAA and 387 Hz between NAA-tCre/tCho. Transition bands were chosen relatively large (198 Hz) because of the short duration of the pulse. The resonances were refocused with a pair of 4-ms frequency-swept quadratic-phase π pulses with a 4-kHz passband to facilitate sharp transitions (32). A variable delay (τ) was placed symmetrically within this double spin echo (SE) (19) scheme, which although not an outright Carr-Purcell-Meiboom-Gill sequence, provides a more complete refocusing than a simple Hahn echo sequence. Metabolic T_2 measurements were performed by varying τ times, resulting in the following 14 echo times: 58, 66, 74, 82, 94, 110, 126, 142, 158, 178, 198, 218, 234, and 254 ms. These were played out in a random order to avoid any bias-related artifacts. The repetition time (TR) was set to 7.2 s such that all metabolites, whose T_1 values at this field range between 1–1.7 s (13) were fully relaxed during signal averaging. With 16 averages per TE, each scan took 1 min and 52 s to acquire, resulting in ~26-min scan time for a full T_2 measurement. A three-dimensional (3D) localization module was applied over both a stroked (ipsilateral) and a comparable healthy region on the contralateral side using LASER (33). This module was 42-ms long, and involved three pairs of 5-ms adiabatic π pulses with an 18-kHz bandwidth flanked by crusher gradients. The ensuing voxel dimensions were 4.8 mm^3. Additionally, water T_2 was measured with a PRESS sequence in four naïve animals using the same voxel size and position. The TR was 7.2 s, and 10 echo times were incremented from 14–88 ms.

MR Imaging and Image Processing

All animals were imaged with the homebuilt quadrature surface RF coil in Figure 1a using respiratory monitoring and gating. The placements of each respective voxel were identified with T_2-weighted SE scout images using an MRI sequence with an identical 3D LASER module as that in the subsequent RE-MRS scan but with water-centered pulses. Effort was taken to create a homogenous B_0 field (Full width half maximum (FWHM) < 40 Hz) within each respective voxel by manual adjusting first and second-order shims as well as z^3 and z^4 corrections on the localized water signal.

Following apodization and transformation, signal intensities from the frequency domain spectra for each respective metabolite and TE were extracted using TopSpin software (Bruker-Biospin, Billerica, Massachusetts) and fitted to an exponential decay function using Sigma Plot 11.0 (Systat Software, San Jose, California). Volumetric measurements of the stroke region were done with AMIRA (FEI Visualization Sciences Group, Houston, Texas) by manually tracing the edge of the stroke. Experimental data are presented as mean ± one standard deviation. Statistical analysis was performed by using a one-way analysis of variance and Tukey's post hoc test (SPSS20, IBM, Chicago Illinois). For pairwise comparison, a paired Student's t-test was performed. Statistical significance was accepted at $P < 0.05$.

RESULTS

Quadrature Coil Performance at 21.1. T

Measured in-magnet and while loaded with an anesthetized 230-g rat, the Q value (34) of the structure in Figure 1a was 171 and 184 for each of the individual coils that make up the quadrature design. The resulting in vivo ^{1}H image SNR (measured on a medially located single image slice, $n=8$) was 25.3 ± 5.7. By comparison, a linear birdcage coil loaded with physiologically relevant sample produces a measured Q value of 49, and has an in vivo ^{1}H image SNR of 15.0 ± 3.1 ($n=7$), representing a significantly lower SNR compared with the quadrature saddle ($P = 0.001$). All of the variable capacitors of the homebuilt quadrature design were externally tunable except for the single decoupling capacitor, which was kept at a constant value for all experiments. As a result, the coil was somewhat sensitive to differences in loading. Careful attention therefore was paid to the placement and alignment of the animal. Figure 2 shows B_1 flip maps collected on a polyethylene glycol phantom (Fig. 2a–2b), and in vivo on a rat at a central slice (Fig. 2c), displaying in both cases the flip angle distribution. The in vivo B_1 flip map reveals a homogeneous B_1 field in which the localized voxels are placed but also a narrow area of optimal flip angles for the two hemispheres, pointing out the importance of animal positioning in the coil.

^{1}H Spectral Acquisition

Figure 3 shows representative ^{1}H spectra, together with the 3D LASER localization regions highlighted on the ^{1}H images. The stroke can be seen as a hyperintense signal in the right hemisphere, as expected from T_2-weighted MRI at 24 h post-ischemia. The RE-MRS sequence generates high-quality spectra (Fig. 3), with only the four targeted metabolites apparent. No evidence of contamination by other metabolic resonances is observed, with a nearly complete absence of the ~10,000 times more intense water resonance and a very flat baseline. These factors are a consequence of the sequence's pulse selectivity, the high spectral dispersion endowed by the high fields, and the relatively fast decay of nontargeted resonance (eg, those of superimposed macromolecules). Average SNR are shown for the targeted metabolites in Figure 3 for the shortest TE assayed (58 ms); the effect on NAA and Lac after transient ischemia is clearly visible, reflecting the anaerobic metabolic activity and decreased neuronal

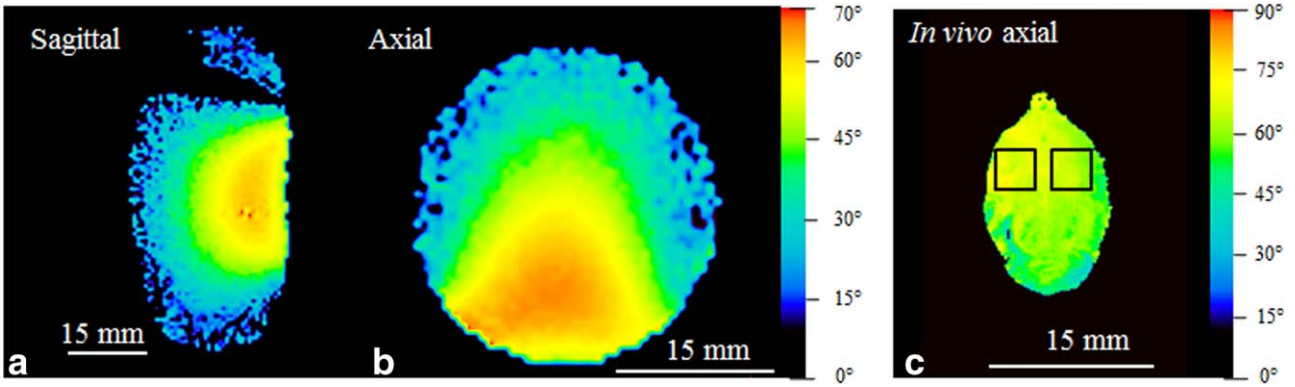

FIG. 2. B_1 tip angle maps of sagittal (a) and axial (b) orientations collected on a polyethylene glycol sample, which provides a similar loading as an in vivo rat. (c) Anatomical B_1 map in vivo; the two squares show the approximate spatial locations of the RE-MRS voxels used in this study.

viability in the stroked region. With only 16 averages requiring less than 2 min of acquisition time, the average contralateral SNR ranged from 9 ± 2 (Lac) to 60 ± 12 (tCre) for all metabolites. This SNR facilitates the robust determination of metabolic T_2s in both healthy and stroked tissue. Stacked plots in Figures 3d and 3e demonstrate the quality of the spectra for all acquired TEs. In general, signals exhibit the expected single exponential signal decay, although contralateral-side tCre and NAA resonances may hint at alternate (sigmoidal or Gaussian) decay profiles, which could be caused by heterogeneities in the target voxel that introduce a degree of chemical-shift dispersion that becomes apparent at very high fields. These heterogeneities might also explain the varying linewidths observed as a function of decay time.

T_2 Measurements

These features notwithstanding, when signal intensities for each metabolite and hemisphere are plotted against TE, reliable single exponential decay curves are obtained. The solid lines in Figures 4a and 4b show the fitting of individual metabolite data to single exponential decay functions, leading to the T_2 values shown in the insets. The goodness values of these fits are >94% (Adj R^2) for all metabolites. A benefit of the RE-MRS approach is that the doublet Lac resonance at 1.33 ppm remains in phase throughout these TE-dependent measurements (as evident from the absence of any J-coupling induced signal oscillations upon varying TE) without performing a Carr-Purcell-Meiboom-Gill excitation or

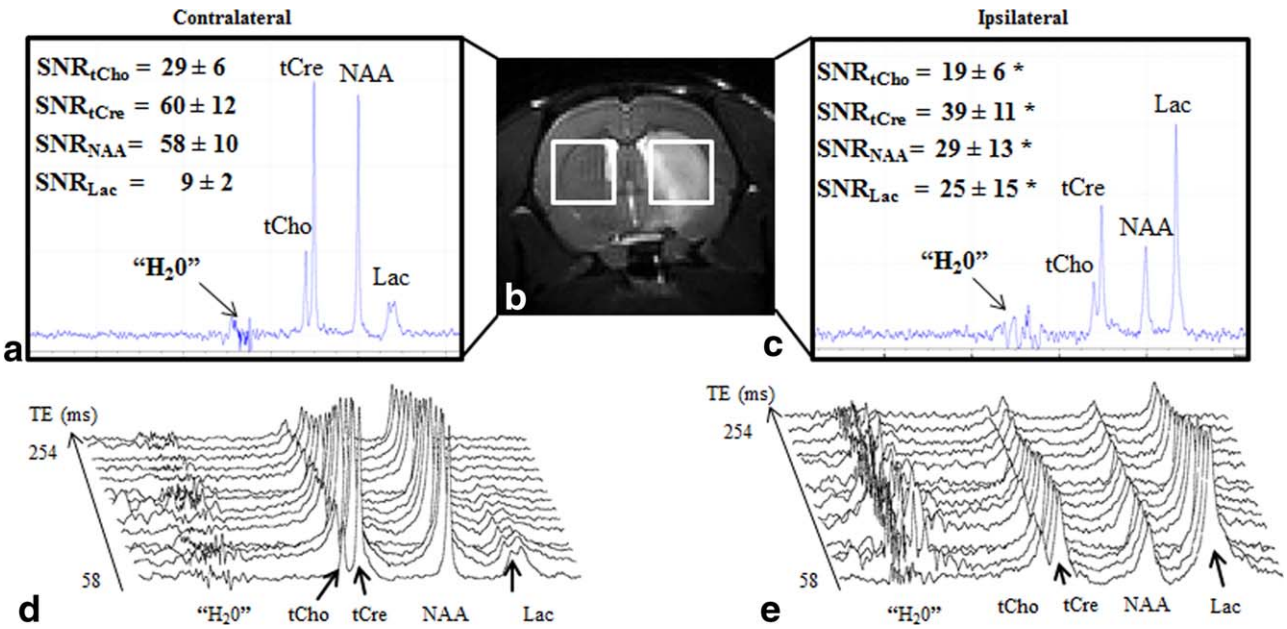

FIG. 3. Representative RE-MRS spectra (magnitude mode representation) generated for the shortest TE assayed (58 ms), showing the average SNR of each metabolite on the contralateral (a) and ipsilateral (c) side of the stroke, after 16 averages. * indicates a significant decrease (tCho, tCre, and NAA) or increase (Lac) of each metabolite respective to the contralateral side, according to the Student's t-test ($P < 0.05$). (b) T_2-weighted image with each respective localized voxel (illustrated with white squares). Representative stack plots from all acquired TEs are shown from the contralateral (d) and ipsilateral (e) hemispheres.

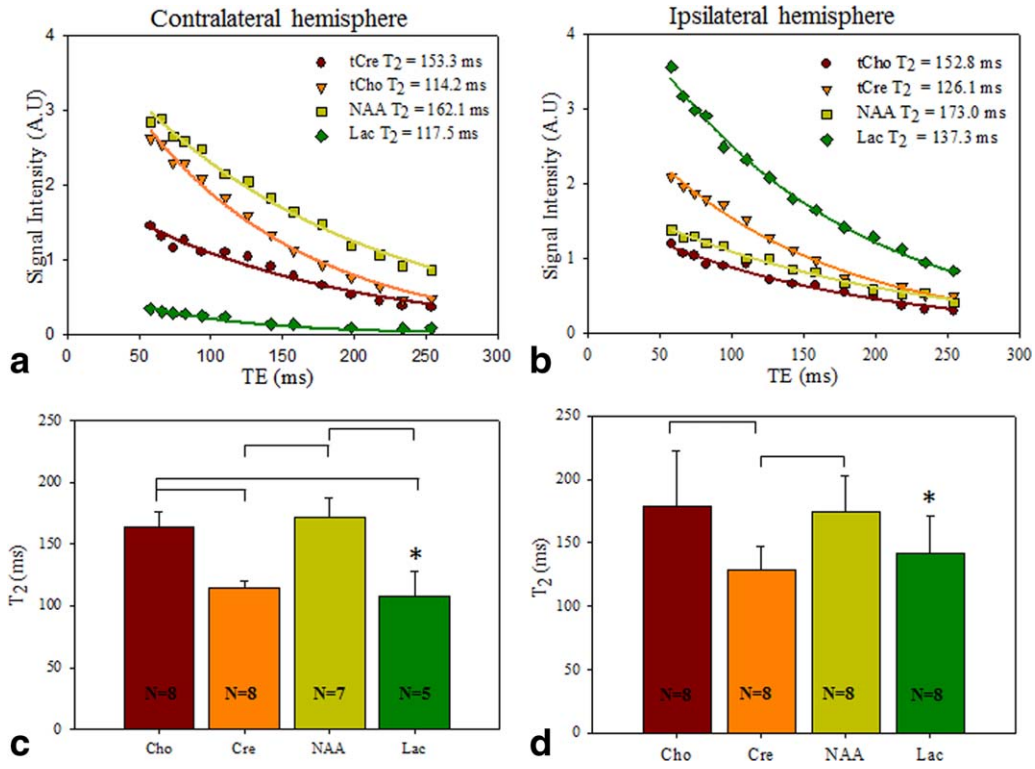

FIG. 4. Representative signal-intensity plots of the targeted metabolites versus TE (ms) on the contralateral (a) and the ipsilateral (b) hemispheres. Average apparent T_2 behavior on the contralateral (c) and ipsilateral (d) hemispheres for eight animals. Because of low concentrations of Lac in three of the eight animals on the contralateral hemisphere, $n = 5$ for this metabolite. Lac is the only metabolite showing a significant increase between contra- and ipsi-lateral hemispheres according to the Student's t-tests ($P < 0.05$) and indicated with *. Brackets indicate significant differences among metabolites by one-way analysis of variance and Tukey's post hoc test ($P < 0.05$). Error bars indicate +/− 1 standard deviation.

specialized phase-cycling scheme. This J-independent decay arises from the spectral profiles of the RF pulses, which refocus the targeted Lac methyl peak but avoid inversion of its coupled methine partner, resulting in a J-echo at all TEs. The Lac resonance (1.33 ppm) at short TE times and the low Lac concentration of the contralateral hemisphere (Fig. 3d) occasionally can have the appearance of a doublet. Rather than representing the actual J-coupling of lactate at this location, the additional upfield resonance likely originates from macromolecular lipid resonances that are more prominent at shorter TE and with low Lac levels. These lipid resonances disappear at longer TE values.

The lower panels of Figure 4 show the average T_2 relaxation times for each respective metabolite on the ipsi- and contralateral hemispheres. Metabolic T_2s measured were markedly longer than typical water values, which were measured at 21.1 T to be 20.7 ± 0.2 ms ($n = 4$). The metabolic T_2s measured here were 179, 129, 175, and 142 ms for tCho, tCre, NAA and Lac, respectively, on the ipsilateral hemisphere, and 164, 115, 172, and 108 ms, respectively, for the contralateral hemisphere. Significant differences are observed between the four metabolites on each respective hemisphere, as indicated by brackets in Figures 4c and 4d. Although all metabolites show average increases in apparent T_2 when comparing the ipsilateral hemisphere to the contralateral, Lac is the only metabolite displaying a statistically significant increase ($P = 0.007$). The NAA from one animal was not able to be T_2-fitted for all TEs and was excluded. Likewise for Lac, the low concentration on the contralateral side and low signal with long TEs prevented accurate curve fitting on three of the eight animals as indicated in Figure 4c.

To assess the effects of variability in lesion size and ensuing partial volume effects, Pearson's correlation factor was calculated. No clear trends between lesion size and T_2s could be determined except for tCre, which showed a weak linear increase of 0.56 with increased stroke lesion.

DISCUSSION

To exploit in vivo MRI and MRS at ultra-high fields, specialized hardware and customized sequences must be explored to take full advantage of the benefits of field strength, while avoiding the disadvantages of high frequency operation. This study presents a step in that direction with the implementation of a quadrature surface-coil design operating at 900 MHz and accommodating relatively large rodents; the in vivo SNR of this quadrature design was 67% higher than the linear birdcage coil that was sized to accommodate the living rat head. The quadrature and saddle implementations also improved the B_1 homogeneity over a flat surface coil, thanks to an optimized aspect ratio and azimuthal coverage (35). As shown in Figure 2c, the resulting B_1 field

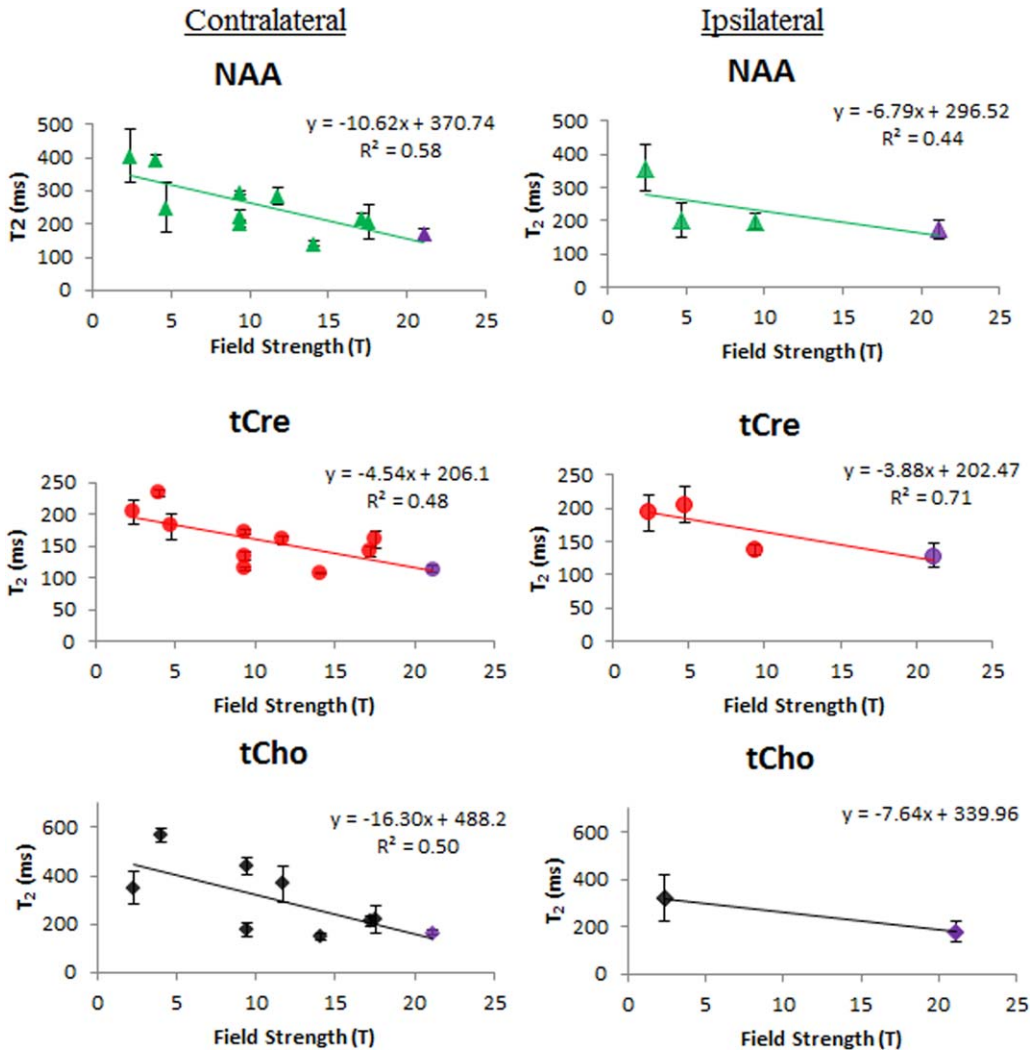

FIG. 5. Comparison between the apparent T_2 relaxation values measured in this study at 21.1 T (purple dots) against similar data acquired at lower field strengths (10,11,14,21–25). The metabolic relaxation times are plotted versus respective field strengths for either healthy controls or contralateral hemispheres and the stroked ipsilateral hemisphere in ischemic studies. Error bars indicate +/− 1 standard deviation.

shows good uniformity within the localized voxels. This efficiency is required for the LASER localization modules and by the relatively long pulse lengths needed by the RE-MRS sequence. Thus, the combination of an efficient quadrature surface coil and customized sequence delivered high SNRs and RF efficiency, enabling the execution of quality, spatially localized RE-MRS experiments at 21.1 T.

Thus equipped, a series of quantitation analyses and T_2 measurements were implemented on selected metabolites of rats subject to MCAO. The localized RE-MRS sequence implemented at 21.1 T provided spectra (Fig. 3) that hint at the metabolic events that occur after ischemia. The significant increase in Lac SNR in the stroked region arises from anaerobic metabolism, including increased anaerobic glycolysis and decreased Lac clearance rate (6,36,37). The significant SNR decrease ($P = 0.0002$) of NAA reflects the impaired neuronal viability or temporary shutdown of its synthesis (38–40), whereas the significant decreases in Cho and Cre SNRs ($P = 0.007$ and 0.003) probably reflect reduced membrane lipid synthesis and altered energetics (7,41,42). These changes are reflected in other studies that compare metabolites in the MCAO animal model (43–46).

Compared with studies of control or contralateral (ie, nonischemic) brain hemispheres at lower fields (10,11,14,21–25), the RE-MRS measurements on the contralateral hemispheres showed a further decrease in T_2 at 21.1 T. Indeed, although a spread of metabolic T_2 values in ^{1}H MRS may arise as a result of different times elapsed between the MCAO and MR scanning or from the specifics of the acquisition technique used (chemical shift imaging (CSI) versus voxel selective, with and without J-coupling suppression), a clear linear decrease in metabolic T_2 versus field strength is evident for preclinical rodent brains. Literature (Fig. 5) reveals that average values of 359, 193, and 322 ms at 2.35 T (21) for NAA, Cre and Cho, respectively, change to 206, 160, and 222 ms, respectively, at 17.6 T (24). These values are all higher than the ones measured in the current 21.1T

study. Even so, all metabolic T_2 values at 21.1 T exceed 100 ms, providing ample opportunity for the use of RE-MRS not only to enhance sensitivity but to investigate techniques, such as diffusion and multiple quantum coherences that require long effective echo times. With regard to water T_2, there is a general trend in shortened T_2 with increasing magnetic field strength, which was measured to be 20.6 ± 0.2 ms at 21.1 T. By comparison, at 3 T, water T_2 is 75 ± 2 ms (47), whereas at 17.2 T (25), a relaxation time of 26 ± 2 ms has been reported. Plots comparing metabolic T_2 between fields in Figure 5 for NAA, tCre, and tCho (10,11,14,21–25) also show such trends. Only one previous study has measured T_2 of Lac in healthy tissue (25). This study measured a T_2 of 218 ± 17 ms at 17.2 T, which falls within the range measured here. Notably, with spectral fidelity and avoidance of water excitation, the RE-MRS approach and resultant high SNR per unit time allow for nearly twice as many TE values to be sampled as conventionally reported and over shorter total experimental times, which could have methodological ramifications and biological benefits that may affect the more complicated aspects (ie, exchange and compartmentalization) of T_2 relaxation interpretation.

Metabolic T_2 relaxation times may yield valuable insight into the ischemic region of stroke. However, literature displays a spread in metabolic T_2s in ischemic lesions compared with healthy control or contralateral tissue. Although not impairing a clear trend of shorter average ischemic metabolic T_2s versus magnetic field (Fig. 5) (10,11,14,21–25), this scatter surely reflects the time elapsed since ischemia and/or the intensity of the MCAO. At 2.35 T (21), no significant T_2 changes were identified for any metabolite over 2 h post-ischemia, but at 4.7 T (11), tCre T_2 showed a significant increase 24-h post-ischemia. At 9.4 T (14), NAA T_2 showed a significant decrease at 1–1.5 h post-ischemia. In general, the average apparent metabolic T_2 values decrease or remain constant with the onset of ischemia. Likewise, the metabolic T_2 values reported in this 21.1T study do not show significant differences between ipsilateral or contralateral hemispheres at 24-h post-ischemia for NAA, tCho and tCre, with average T_2s increasing only slightly. Lac, by contrast, shows a significant increase in its T_2. Notably, none of the aforementioned studies reports such an increase in Lac T_2, likely because of low Lac concentrations in healthy tissue. The RE-MRS approach now provides enough SNR to be measured in the contralateral hemisphere even at echo times $TE \geq 250$ ms, which admittedly was more difficult in healthy tissue. This ability to measure metabolic T_2 values at 21.1 T would facilitate the absolute quantification of concentration changes resulting from ischemia, and support the use of advanced RE-MRS techniques to classify stroke conditions.

In addition to T_2 scatter arising from the time elapsed post-ischemia, care should be taken when quantitatively comparing T_2 values of different studies: Stroke severity and size, for instance, could also affect the measured values. Additional factors that could influence this change in transverse relaxation time include the presence of edema, metabolite binding to macromolecules (48), and macromolecular breakdown during evolution of stroke, resulting in altered metabolic binding sites (49). In addition, just as changes in water T_2 relaxation with ischemic injury are closely linked to the apparent diffusion coefficient and altered extra/intracellular space distributions (10), apparent metabolic T_2s investigated by RE-MRS are likely affected in environments that also hinder or restrict diffusion (20). The analysis by which the experimental points are fitted (mono- versus biexponential) could also influence the results; this has been reported for tCre in the primary visual cortex in humans (50), but no such differences were observed in this study.

In the current implementation, RE-MRS produces undistorted peaks and artifact-free baselines. A drawback of this approach, which uses highly selective pulses and the LASER sequence for localization, is its relatively long initial TE of 58 ms. Although other MRS studies (22) have used medium to long TEs to avoid the effect of macromolecular signals, there is the potential for loss of information about short T_2 components of these and other metabolites. RE-MRS experiments involving other localization schemes, including chemical shift imaging, could be used to assess shorter TE values. As with any study, partial-volume effects are also limiting factors to the accurate measurement of T_2 trends; future work will be aimed at smaller, more focused voxels to reduce variability and probe regional metabolic differences within the ischemic lesion volume (51). Other metabolites, such as glutamine, glutamate and myo-inositol, are also of relevance for stroke. The sensitivity and fidelity of the RE-MRS sequence coupled with ultra-high magnetic fields and optimized RF coils could facilitate the study of these more challenging metabolites, even if these targets may call for the use of far more sophisticated multiband pulses.

In conclusion, a quadrature RF coil and the RE-MRS sequence were employed to investigate selectively excited metabolites at 21.1 T, revealing a reduction in apparent metabolic T_2 relaxation compared with lower field strengths (10,24,25) and a slight trend of longer metabolic T_2 at 24 h post-ischemia within the lesion (14,21). With this feature and the SNR afforded by RE-MRS at ultra-high fields, these relatively long metabolic T_2s enable several other potential investigations, including metabolic diffusion, cellular compartmentalization, and multiple quantum studies. As a result, knowledge about metabolic T_2 relaxation times at high field is important both from a fundamental perspective and from a more applicative approach concerning the design and optimization of sequences aimed at metabolic MRS and the evaluation of disease states.

ACKNOWLEDGMENTS

The authors would like to thank Ashley Blue and Fabian Calixto Bejarano for technical assistance. This work was performed at the National High Magnetic Field Laboratory, which is supported by NSF DMR-1157490 and the State of Florida. Funding was also provided by the NHMFL User Collaboration Grants Program (to SGC) and the American Heart Association Grant-in-Aid program (10GRNT3860040). The authors also wish to thank the Israel Science Foundation (Grants ISF 795/13 and 1142/

13), the Kimmel Institute for Magnetic Resonance, and the generosity of the Perlman Family Foundation (to LF). NS acknowledges a Visiting Scientist Program grant (NHMFL 12601). LF and SCG contributed equally to this study.

REFERENCES

1. Heiss W. The concept of the penumbra: can it be translated to stroke management? Int J Stroke 2010;5(4):290–5.
2. Moseley ME, de Crespigny AJ, Roberts TP, Kozniewska E, Kucharczyk J. Early detection of regional cerebral ischemia using high-speed MRI. Stroke 1993;24(12 Suppl):I60–I65.
3. Moseley ME, Wendland MF, Kucharczyk J. Magnetic resonance imaging of diffusion and perfusion. Top Magn Reson Imaging 1991;3(3): 50–67.
4. Kucharczyk J, Mintorovitch J, Asgari HS, Moseley M. Diffusion/perfusion MR imaging of acute cerebral ischemia. Magn Reson Med 1991; 19(2):311–315.
5. Soares DP, Law M. Magnetic resonance spectroscopy of the brain: review of metabolites and clinical applications. Clin Radiol 2009; 64(1):12–21.
6. Lei H, Berthet C, Hirt L, Gruetter R. Evolution of the neurochemical profile after transient focal cerebral ischemia in the mouse brain. J Cereb Blood Flow Metab 2009;29(4):811–819.
7. Duarte JM, Lei H, Mlynarik V, Gruetter R. The neurochemical profile quantified by in vivo 1H NMR spectroscopy. NeuroImage 2012;61(2): 342–362.
8. Bonavita S, Di Salle F, Tedeschi G. Proton MRS in neurological disorders. Eur J Radiol 1999;30(2):125–131.
9. Ricci PE Jr. Proton MR spectroscopy in ischemic stroke and other vascular disorders. Neuroimaging Clin N Am 1998;8(4):881–900.
10. de Graaf RA, Brown PB, McIntyre S, Nixon TW, Behar KL, Rothman DL. High magnetic field water and metabolite proton T1 and T2 relaxation in rat brain in vivo. Magn Reson Med 2006;56(2):386–394.
11. van der Toorn A, Dijkhuizen RM, Tulleken CA, Nicolay K. T1 and T2 relaxation times of the major 1H-containing metabolites in rat brain after focal ischemia. NMR Biomed 1995;8(6):245–252.
12. Cudalbu C, Mlynarik V, Xin L, Gruetter R. Comparison of T1 relaxation times of the neurochemical profile in rat brain at 9.4 Tesla and 14.1 Tesla. Magn Reson Med 2009;62(4):862–867.
13. Shemesh N, Rosenberg JT, Dumez JN, Grant SC, Frydman L. Metabolic T_1 dynamics and longitudinal relaxation enhancement in vivo at ultrahigh magnetic fields on ischemia. J Cereb Blood Flow Metab 2014;34:1810–8017.
14. Lei H, Zhang Y, Zhu XH, Chen W. Changes in the proton T2 relaxation times of cerebral water and metabolites during forebrain ischemia in rat at 9.4 T. Magn Reson Med 2003;49(6):979–984.
15. Ogawa S, Menon RS, Tank DW, Kim SG, Merkle H, Ellermann JM, Ugurbil K. Functional brain mapping by blood oxygenation level-dependent contrast magnetic resonance imaging. A comparison of signal characteristics with a biophysical model. Biophys J 1993;64(3): 803–812.
16. Zhu XH, Chen W. Observed BOLD effects on cerebral metabolite resonances in human visual cortex during visual stimulation: a functional (1)H MRS study at 4 T. Magn Reson Med 2001;46(5):841–847.
17. Michaeli S, Garwood M, Zhu XH, DelaBarre L, Andersen P, Adriany G, Merkle H, Ugurbil K, Chen W. Proton T2 relaxation study of water, N-acetylaspartate, and creatine in human brain using Hahn and Carr-Purcell spin echoes at 4T and 7T. Magn Reson Med 2002;47(4):629–633.
18. Rosenberg JT, Sachi-Kocher A, Davidson MW, Grant SC. Intracellular SPIO labeling of microglia: high field considerations and limitations for MR microscopy. Contrast Media Mol Imaging 2012;7(2):121–129.
19. Shemesh N, Dumez JN, Frydman L. Longitudinal relaxation enhancement in 1H NMR spectroscopy of tissue metabolites via spectrally selective excitation. Chemistry 2013;19(39):13002–13008.
20. Shemesh N, Rosenberg JT, Dumez JN, Muniz JA, Grant SC, Frydman L. Metabolic properties in stroked rats revealed by relaxation-enhanced magnetic resonance spectroscopy at ultrahigh fields. Nat Comm 2014;5:4958.
21. Fujimori H, Michaelis T, Wick M, Frahm J. Proton T2 relaxation of cerebral metabolites during transient global ischemia in rat brain. Magn Reson Med 1998;39(4):647–650.
22. Xin L, Gambarota G, Mlynarik V, Gruetter R. Proton T2 relaxation time of J-coupled cerebral metabolites in rat brain at 9.4 T. NMR Biomed 2008;21(4):396–401.
23. Xin L, Gambarota G, Cudalbu C, Mlynarik V, Gruetter R. Single spin-echo T2 relaxation times of cerebral metabolites at 14.1 T in the in vivo rat brain. MAGMA 2013;26(6):549–554.
24. Weiss K, Melkus G, Jakob PM, Faber C. Quantitative in vivo 1H spectroscopic imaging of metabolites in the early postnatal mouse brain at 17.6 T. MAGMA 2009;22(1):53–62.
25. Lopez-Kolkovsky AL, Mériaux S, Boumezbeur F. Metabolite and macromolecule T1 and T2 relaxation times in the rat brain in vivo at 17.2T. Magn Reson Med. 2016;75:503–514.
26. Fu R, Brey WW, Shetty K, et al. Ultra-wide bore 900 MHz high-resolution NMR at the national high magnetic field laboratory. J Magn Reson 2005;177(1):1–8.
27. Cunningham CH, Pauly JM, Nayak KS. Saturated double-angle method for rapid B1+ mapping. Magn Reson Med 2006;55(6):1326–1333.
28. Longa EZ, Weinstein PR, Carlson S, Cummins R. Reversible middle cerebral artery occlusion without craniectomy in rats. Stroke 1989; 20(1):84–91.
29. Rosenberg JT, Sellgren KL, Sachi-Kocher A, Calixto Bejarano F, Baird MA, Davidson MW, Ma T, Grant SC. Magnetic resonance contrast and biological effects of intracellular superparamagnetic iron oxides on human mesenchymal stem cells with long-term culture and hypoxic exposure. Cytotherapy 2013;15(3):307–322.
30. Leftin A, Rosenberg JT, Solomon E, Calixto Bejarano F, Grant SC, Frydman L. Ultrafast in vivo diffusion imaging of stroke at 21.1 T by spatiotemporal encoding. Magn Reson Med 2015;73(4):1483.
31. Pauly J, Le Roux P, Nishimura D, Macovski A. Parameter relations for the shinnar-le roux selective excitation pulse design algorithm [NMR imaging. IEEE Trans Med Imaging 1991;10(1):53–65.
32. Schulte RF, Tsao J, Boesiger P, Pruessmann KP. Equi-ripple design of quadratic-phase RF pulses. J Magn Reson 2004;166(1):111–122.
33. Garwood M, DelaBarre L. The return of the frequency sweep: designing adiabatic pulses for contemporary NMR. J Magn Reson 2001; 153(2):155–177.
34. Qian C, Masad IS, Rosenberg JT, Elumalai M, Brey WW, Grant SC, Gor'kov PL. A volume birdcage coil with an adjustable sliding tuner ring for neuroimaging in high field vertical magnets: ex and in vivo applications at 21.1 T. J Magn Reson 2012;221:110–116.
35. Salmon CEG, Vidoto ELG, Martins MJ, Tannus A. Optimization of saddle coils for magnetic resonance imaging. Braz J Phys 2006;36(1A):4–8.
36. Kuhr WG, van den Berg CJ, Korf J. In vivo identification and quantitative evaluation of carrier-mediated transport of lactate at the cellular level in the striatum of conscious, freely moving rats. J Cereb Blood Flow Metab 1988;8(6):848–856.
37. Walz W, Mukerji S. Lactate release from cultured astrocytes and neurons: a comparison. Glia 1988;1(6):366–370.
38. Demougeot C, Bertrand N, Prigent-Tessier A, Garnier P, Mossiat C, Giroud M, Marie C, Beley A. Reversible loss of N-acetyl-aspartate in rats subjected to long-term focal cerebral ischemia. J Cereb Blood Flow Metab 2003;23(4):482–489.
39. Demougeot C, Garnier P, Mossiat C, Bertrand N, Giroud M, Beley A, Marie C. N-acetylaspartate, a marker of both cellular dysfunction and neuronal loss: its relevance to studies of acute brain injury. J Neurochem 2001;77(2):408–415.
40. Shemesh N, Sadan O, Melamed E, Offen D, Cohen Y. Longitudinal MRI and MRSI characterization of the quinolinic acid rat model for excitotoxicity: peculiar apparent diffusion coefficients and recovery of N-acetyl aspartate levels. NMR Biomed 2010;23(2):196–206.
41. Federico F, Simone IL, Lucivero V, Giannini P, Laddomada G, Mezzapesa DM, Tortorella C. Prognostic value of proton magnetic resonance spectroscopy in ischemic stroke. Arch Neurol 1998;55(4):489–494.
42. Kang B, Jang D, Lee J, et al. Detection of cerebral metabolites in a canine model of ischemic stroke using 1H magnetic resonance spectroscopy. Res Vet Sci 2009;87(2):300–306.
43. Berthet C, Xin L, Buscemi L, Benakis C, Gruetter R, Hirt L, Lei H. Non-invasive diagnostic biomarkers for estimating the onset time of permanent cerebral ischemia. J Cereb Blood Flow Metab 2014;34(11): 1848–1855.
44. Qian J, Qian B, Lei H. Reversible loss of N-acetylaspartate after 15-min transient middle cerebral artery occlusion in rat: a longitudinal study with in vivo proton magnetic resonance spectroscopy. Neurochem Res 2013;38(1):208–217.

45. Alf MF, Lei H, Berthet C, Hirt L, Gruetter R, Mlynarik V. High-resolution spatial mapping of changes in the neurochemical profile after focal ischemia in mice. NMR Biomed 2012;25(2):247–254.
46. Berthet C, Lei H, Gruetter R, Hirt L. Early predictive biomarkers for lesion after transient cerebral ischemia. Stroke 2011;42(3): 799–805.
47. Aradi M, Steier R, Bukovics P, Szalay C, Perlaki G, Orsi G, Pal J, Janszky J, Doczi T, Schwarcz A. Quantitative proton MRI and MRS of the rat brain with a 3T clinical MR scanner. J Neuroradiol 2011;38(2): 90–97.
48. Leibfritz D, Dreher W. Magnetization transfer MRS. NMR Biomed 2001;14(2):65–76.
49. Graham GD, Hwang JH, Rothman DL, Prichard JW. Spectroscopic assessment of alterations in macromolecule and small-molecule metabolites in human brain after stroke. Stroke 2001;32(12):2797–2802.
50. Ke Y, Cohen BM, Lowen S, Hirashima F, Nassar L, Renshaw PF. Biexponential transverse relaxation (T(2)) of the proton MRS creatine resonance in human brain. Magn Reson Med 2002;47(2):232–238.
51. Weber R, Ramos-Cabrer P, Justicia C, Wiedermann D, Strecker C, Sprenger C, Hoehn M. Early prediction of functional recovery after experimental stroke: functional magnetic resonance imaging, electrophysiology, and behavioral testing in rats. J Neurosci 2008;28(5): 1022–1029.